mathematics

MDPI

Article

Research on Vibration Propagation Law and Dynamic Effect of Bench Blasting

Lu He [1,2], Dezhong Kong [2,3,*] and Zhen Lei [4]

[1] School of Energy and Mining Engineering, China University of Mining and Technology-Beijing, Beijing 100083, China
[2] College of Mining, Guizhou University, Guiyang 550025, China
[3] State Key Laboratory of Public Big Data, Guizhou University, Guiyang 550025, China
[4] School of Mining Engineering, Guizhou Institute of Technology, Guiyang 550003, China
* Correspondence: dzkong@gzu.edu.cn

Abstract: To address the problem of damage to adjacent buildings (structures) caused by bench blasting construction, blasting in a sand and gravel mine in Guizhou Province was used as the background. Through on-site monitoring and numerical simulation, the blasting vibration propagation law and dynamic effect characteristics under the joint action of different bench heights and horizontal distances were studied. The regression model was established. The results show that: the peak vibration speed in all three directions with the increase in the horizontal distance of the burst center is a decaying trend, and the field measurements are basically consistent with the safe vibration speed and do not exceed 1.5 cm/s, so the house is in a safe state; shear stress with the increase in the horizontal distance of the burst center strictly decays, so the source of the shear stress and vibration speed decay faster in the near zone, with the slow decay in the far zone; analysis found that the shear stress and vibration speed are quadratic and exponential. Through the analysis of the regression model, it is obtained that there is no co-linearity among the influencing factors, which has a significant effect on the regression equation and regression coefficient, and so the multiple linear regression equation fits well. The model can predict the blast vibration intensity, which can be used as a safety criterion for buildings under the action of blasting, and provides a reference for blast vibration control, hole network parameters, and the design index.

Keywords: beach blasting; field monitoring; numerical simulation; propagation law; dynamic effect

MSC: 65E05

Citation: He, L.; Kong, D.; Lei, Z. Research on Vibration Propagation Law and Dynamic Effect of Bench Blasting. *Mathematics* **2022**, *10*, 2951. https://doi.org/10.3390/math10162951

Academic Editors: Ioannis Dassios and Clemente Cesarano

Received: 17 July 2022
Accepted: 13 August 2022
Published: 16 August 2022

1. Introduction

In open pit mining, road excavation, and other slope projects, bench blasting excavation technology can significantly improve the construction efficiency and velocity of the project progress. However, the bench blasting vibration effect seriously affects the safety of the surrounding buildings (structures) and the stability of the rock structure of the slope. Theoretical analyses, field tests, and numerical simulations have been used to research bench blasting vibration. To clarify the impact of blast vibration on buildings and provide a reference basis for blast vibration control and prediction of whether the structure is damaged, based on Sadovsky's empirical formula, experts have proposed an elevation correction formula considering the high slope conditions.

In recent years, scholars at home and abroad have mainly focused on the vibration velocity of blasting seismic waves. The empirical formulae for the variation of blasting vibration velocity with explosive quantity and blast core distance have been summarized by using the method for dimensional analysis, and the prediction and assessment of blast vibration have been carried out accordingly [1–3]. In terms of the propagation law of blasting vibration, Yin et al. [4] investigated the attenuation law of blast vibration waves in

nodal slopes using blast vibration signals monitored in situ from the blasting of different rock masses. Yu et al. [5] and Tan et al. [6] studied the blasting vibration variations in the slope areas of mines and reservoir projects and summarized the variations of blasting velocity inside the slope. Li et al. [7] derived the blasting vibration response law of slopes in quarries by the regression analysis of many vibration test data. Wan et al. [8] studied the propagation law of seismic waves in blasting of hydropower station projects through blasting vibration tests. Rafael Rodríguez et al. [9] proposed a user-friendly methodology for determining the behavior of vibrations generated in any rock mass. Zhu et al. [10] proposed a new method to predict the vibration velocity of multi-hole trenching blasting of laminated rock masses, which can be used for optimizing engineering blasting design and the blasting of the slope. In order to study the propagation law of blast vibration in soft rock tunnels, Chen et al. [11] carried out an analysis and research on the measured data by blast vibration tests and used nonlinear regression and Fourier transform methods to provide a reference for the optimization of blast design in the Muzhailing tunnel or similar soft rock tunnels; Lin et al. [12] proposed a superposition prediction method based on the propagation and superposition principles of blast vibration signals; Xiao et al. [13] obtained the slope blasting vibration propagation law by fitting the Sadovsky formula based on field blasting vibration monitoring data; Gao et al. [14] used regression analysis for the Sadovsky and the CRSRI blast vibration velocity prediction models during onsite operations; Zhang et al. [15], through field blasting vibration monitoring and numerical simulation, proposed the propagation law of blasting vibration velocity in the high side wall, elucidated the local elevation amplification effect of blasting vibration velocity, and modified Sadovsky's formula; Tian et al. [16] used MATLAB to compile a signal processing program to analyze the propagation law of blast vibration in the stratum of shallow buried tunnels with oversized cross-sections. In terms of the research of dynamic response. Yan et al. [17] studied the blasting vibration response law of slopes at different elevations by modifying the elevation formula and numerical simulation. Xie et al. [18] used a modified DDA method to study the dynamic response of rocks under blast loads. Deng et al. [19] derived an attenuation formula for the propagation velocity of elastic stress waves in elastomers based on the stress wave theory, which provides a reference for similar excavation blasting and vibration control methods to provide a reference for similar excavation blasting and vibration control methods. The blasting data measured and obtained in the actual project is complicated, time consuming, inconvenient, and has great limitations. Therefore, most scholars use finite element numerical simulation software to analyze the dynamic effect from seismic wave blasting, and then judge whether the buildings are damaged and destroyed from the structural material properties, providing reference for the blasting vibration control, hole network parameters, and design indicators [20–27]. Zhang et al. [28] analyzed the propagation law of vibration in the civil air defense tunnel through field tests and numerical simulations and established a model for the relationship between peak vibration velocity and effective stress; Xu Wu et al. [29] studied, based on theoretical analysis and numerical simulations, the effect of bench height on blasting seismic waves; Yang et al. [30] used numerical simulations to study the vibration characteristics of slopes under blasting loads; Blair et al. [31] used numerical models to study the dynamic response of the shaft wall under blasting loads at the bottom of the shaft wall; Jiang et al. [32] analyzed literature on the study of the dynamic response law of pipelines using field tests, outdoor tests, and numerical simulations. In terms of the impact of blasting vibration on surface buildings, Esmatkhah et al. [33] studied the settlement and damage caused by subway tunnel excavation through onsite monitoring and numerical simulation; Chaudhary et al. [34] conducted a comparative assessment on the performance of conventional and advanced tunnel lining materials subjected to blast loading and used a three-dimensional nonlinear finite element analysis procedure. Tsang et al. [35] presented a practical structural vulnerability assessment method for mine blast-induced vibrations. In general, blast vibration has been studied in-depth and a wealth of research results have been obtained. However, there are few reports on the research on vibration propagation law and the

dynamic effect of bench blasting, and it is not comprehensive enough. Therefore, in order to ensure the safety of surrounding buildings (structures) during blasting, it is necessary to comprehensively and systematically study the vibration propagation laws and dynamic effects under the combined action of horizontal distance and elevation.

In view of this, based on the existing research, field tests and numerical calculations are carried out with the background of a step blasting project in a gravel mine in Guizhou Province, and regression analysis is carried out with the least squares method and SPSS software to study, more comprehensively and systematically, the vibration propagation law and dynamic effect under the joint action of horizontal distance and elevation, to provide a reference basis for controlling blasting vibration and predicting whether the structure is damaged.

2. Basic Theory of Blasting Vibration

2.1. Attenuation Law of Blasting Seismic Wave

Many field measurements and test results show that blasting vibration intensity is closely related to the horizontal distance from the explosive center, charge, geotechnical properties, topographic condition, and other factors. The calculation formula of peak vibration velocity attenuation is Sadovsky's formula recommended in safety regulations for blasting (GB6722-2014) in China.

$$V = K(\frac{\sqrt[3]{Q}}{\mathrm{R}})^{\alpha} \tag{1}$$

It is believed that elevation is an important factor that cannot be ignored in the vibration propagation attenuation law of buildings, and the influence of elevation influence coefficients and blast-related coefficients on blast vibration wave propagation and attenuation cannot be ignored, and so it is urgent to strengthen the research on vibration propagation law. Considering the high side slope conditions, experts from Changjiang River Scientific Research Institute (CRSRI) have proposed an elevation correction formula, as follows.

$$v = K\left(\frac{\sqrt[3]{Q}}{R}\right)^{\alpha}\left(\frac{\sqrt[3]{Q}}{H}\right)^{\beta} \tag{2}$$

In Formulas (1) and (2).

v is particle vibration velocity, cm/s;

Q is the maximum dose, kg;

H is the height difference between explosive source and measuring point, m;

R is the horizontal distance from explosive source to measuring point, m;

K,α are parameters related to terrain and geological conditions;

β is the elevation influence coefficient.

For bench blasting with changing vertical distance from the explosive center, there is stronger compatibility for the formula of the peak vibration velocity propagation law proposed by the elevation correction formula developed by CRSRI. Therefore, the elevation correction formula is used to analyze the field vibration velocity in this study.

The left and right sides of Formula (2) (taking logarithm, respectively) to obtain Formula (3).

$$\lg V = \lg K + \alpha\lg(\frac{\sqrt[3]{Q}}{R}) + \beta\lg(\frac{\sqrt[3]{Q}}{R}) \tag{3}$$

Suppose $z = \lg V$, $a = \lg K$, $b = \alpha$, $x = \lg(\frac{\sqrt[3]{Q}}{R})$, $c = \beta$, $y = \lg(\frac{\sqrt[3]{Q}}{H})$

Then, the Formula (3) can be written

$$Z = a + bx + cy \tag{4}$$

2.2. Influence of Blasting Vibration on Buildings

Suppose the building is considered an elastomer or only its deformation in the elastic phase under blasting. The relationship between stress σ and strain ε when the building (structure) vibrates is as follows.

$$\sigma = E\varepsilon \tag{5}$$

The constant proportionality between stress and strain is known as the coefficient of elasticity or Young's modulus, fixed for different materials. The strain can be obtained according to the particle vibration velocity and the propagation velocity of the seismic wave in the medium.

$$\varepsilon = V/C \tag{6}$$

Thus, the maximum velocity and maximum stress of a mass on a building under the action of a blast seismic wave are proportional to each other. That is, $\sigma_{\max} = \frac{EV_{\max}}{C}$. Therefore, particle vibration velocity can be used to determine the safety of building structures.

3. Field Monitoring and Analysis of Blast Vibration Propagation Law

3.1. Engineering Situations

A sandstone mine in Guizhou Province has good burial conditions and thin overburden and is located above the lowest surface elevation with a bench height of 10 m. The mine blasting scheme uses deep hole blasting, No. 2 rock emulsion explosives, and detonator detonation. Blasting vibration caused by mining needs to be controlled, so blasting vibration monitoring is implemented for the nearest 40 m to 100 m of residential buildings in the blasting operation area from the explosive source.

3.2. Monitoring Content and Methodology

The field test focused on the vibration velocity of blast seismic waves generated during bench blasting at different bench heights and different horizontal distances. The CBSD-VM-M01 digital network vibrator was used for blast vibration testing. The site Monitoring point No.1 layout is shown in Figure 1. Due to space limitations, the site layout plans for the remaining measurement points are not listed.

Figure 1. Monitoring point No.1.

According to the purpose and content of the monitoring and site conditions, five different blasting schemes were used to monitor the site during blasting, with bench heights between 20–60 m and a bench height difference of 10 m. The horizontal distance of the measurement points from the explosive source was 40–100 m, and the horizontal distance of the adjacent measurement points was 15 m. Five monitoring points were arranged for each scheme. Figure 2 shows the layout of the measurement point monitoring scheme for bench heights of 60 m and 20 m. (the unit is m.); other monitoring point layout diagrams are not listed. Table 1 is the monitoring scheme table.

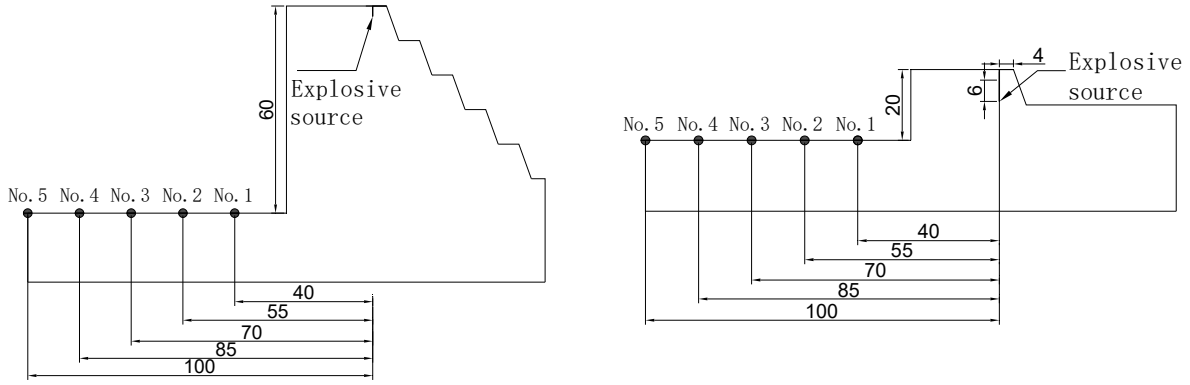

Figure 2. Monitoring scheme for 60 m and 20 m bench height monitoring points. (**a**) Bench height is 60 m. (**b**) Bench height is 20 m.

Table 1. Monitoring scheme.

Monitoring Points	Vertical Distance from the Explosive Center/m	Horizontal Distance from the Explosive Center/m	Slope Angle	Monitoring Content
No. 1	60/50/40/30/20	40	70°	vertical vibration velocity Tangential vibration velocity Radial Vibration Velocity
No. 2		55		
No. 3		70		
No. 4		85		
No. 5		100		

3.3. Monitoring Results

Blasting vibration monitoring was carried out at elevations of 20~60 m blasting. Five fixed measurement points were arranged for each test, and a total of five sets of tests were carried out, with the maximum hazard as the principle, and a set of data on the maximum vibration velocity of the measurement points was taken as the basis of the study. The results of blast vibration monitoring are specified in Table 2.

Table 2. The results of blast vibration monitoring.

Number of Times	Monitoring Point	Horizontal Distance from the Explosive Center /R(m)	Vertical Distance from the Explosive Center /H(m)	Maximum Charge/Q (kg)	Vertical Vibration Velocity/V ($cm \cdot s^{-1}$)	Horizontal Tangent Vibration Velocity/V ($cm \cdot s^{-1}$)	Horizontal Radial Vibration Velocity/V ($cm \cdot s^{-1}$)
1	No.1	40	60	18	0.169	0.170	0.171
	No.2	55			0.160	0.162	0.143
	No.3	70			0.134	0.132	0.120
	No.4	85			0.091	0.092	0.093
	No.5	100			0.086	0.076	0.078

Table 2. *Cont.*

Number of Times	Monitoring Point	Horizontal Distance from the Explosive Center /R(m)	Vertical Distance from the Explosive Center /H(m)	Maximum Charge/Q (kg)	Vertical Vibration Velocity/V ($cm \cdot s^{-1}$)	Horizontal Tangent Vibration Velocity/V ($cm \cdot s^{-1}$)	Horizontal Radial Vibration Velocity/V ($cm \cdot s^{-1}$)
2	No.1	40	50	18	0.183	0.175	0.182
	No.2	55			0.170	0.165	0.156
	No.3	70			0.150	0.149	0.130
	No.4	85			0.109	0.105	0.111
	No.5	100			0.090	0.085	0.095
3	No.1	40	40	18	0.190	0.185	0.187
	No.2	55			0.175	0.171	0.159
	No.3	70			0.154	0.152	0.135
	No.4	85			0.113	0.111	0.115
	No.5	100			0.094	0.096	0.105
4	No.1	40	30	18	0.202	0.195	0.199
	No.2	55			0.176	0.175	0.160
	No.3	70			0.155	0.154	0.139
	No.4	85			0.109	0.119	0.120
	No.5	100			0.088	0.097	0.108
5	No.1	40	20	18	0.248	0.225	0.310
	No.2	55			0.224	0.210	0.250
	No.3	70			0.185	0.180	0.210
	No.4	85			0.169	0.153	0.204
	No.5	100			0.163	0.136	0.184

In the above site monitoring data, the elevation is 20 m and the maximum measured vibration velocity is 0.310 cm/s. According to the safety regulations for blasting (GB6722-2014), the permissible safe vibration velocity of general civil buildings does not exceed 1.5 cm/s, and so the civil house is in a safe state.

3.4. Analysis of Blasting Vibration Propagation Law

3.4.1. Blasting Vibration Attenuation Law

Substitute the data in Table 2 into Equation (4) to find a, b, c using Origin software least-squares multivariate linear algorithm to fit the solution, resulting in an elevation of 20 m. The vertical vibration velocity with the horizontal distance and vertical distance from the explosive center propagation law is as follows.

$$V = 8.60102\left(\frac{\sqrt[3]{Q}}{R}\right)^{0.49546}\left(\frac{\sqrt[3]{Q}}{H}\right)^{1.07416} \quad (7)$$

When the elevation is 20 m, the propagation law of horizontal tangent vibration velocity with horizontal and vertical distance from the explosive center is as follows.

$$V = 9.21000\left(\frac{\sqrt[3]{Q}}{R}\right)^{0.56679}\left(\frac{\sqrt[3]{Q}}{H}\right)^{1.0405} \quad (8)$$

When the elevation is 20 m, the propagation law of horizontal radial vibration velocity with horizontal and vertical distance from the explosive center is as follows.

$$V = 10.28987\,(\frac{\sqrt[3]{Q}}{R})^{0.55874}(\frac{\sqrt[3]{Q}}{H})^{0.98594} \tag{9}$$

When the elevation H = 20 m, the regression diagram of horizontal radial vibration velocity is shown in Figure 3.

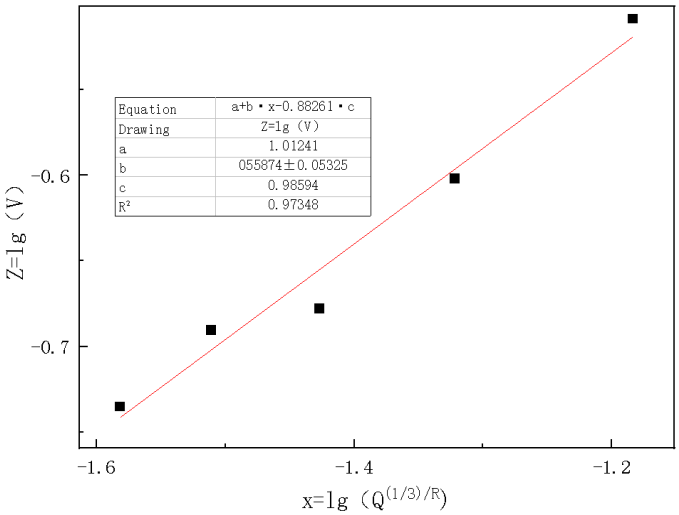

Figure 3. Regression analysis of horizontal radial vibration velocity when the elevation H = 20 m.

We need to obtain the same blast with different vibration velocities of horizontal distance from the explosive center to study the blast vibration peak vibration decay law. However, it is not possible to monitor multiple points because of the limited monitoring equipment. To the principle of maximum hazard, the largest set of five schemes is now taken to approximate the vibration velocity as a blast at different elevations and horizontal locations of vibration velocity. As can be seen from Table 2, the maximum vibration velocity occurs at an elevation of 20 m, the horizontal radial vibration velocity. Therefore, when the elevation is 20 m, the data of the horizontal radial vibration velocity are fitted and analyzed, and the general decay trend of the vibration velocity of the surface residential buildings can be derived, as shown in Figure 4.

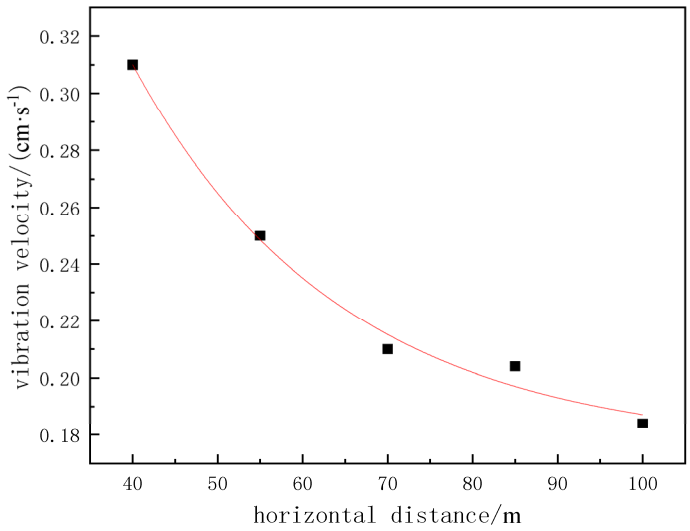

Figure 4. Variation of vibration velocity of surface dwellings with horizontal distance from the explosive center.

As can be seen from Figure 4: the vibration velocity of the surface houses decreases with the increase in the horizontal distance from the explosive center; the overall decay velocity decreases faster in areas closer to the explosive source and becomes slower in areas further away from the source.

From Table 2, the radial, tangential, and vertical vibration velocities are plotted with bench height as shown in Figures 5–7 below.

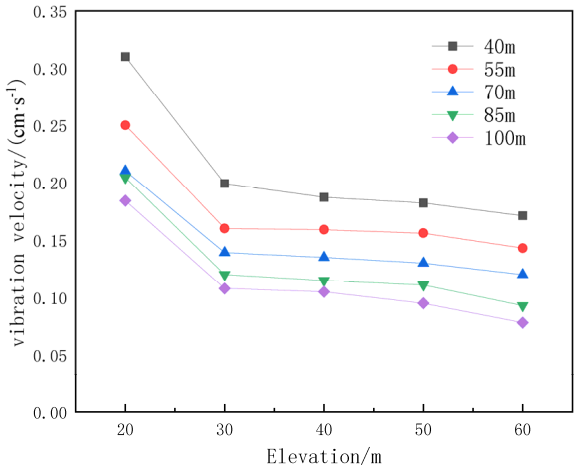

Figure 5. Horizontal radial vibration velocity.

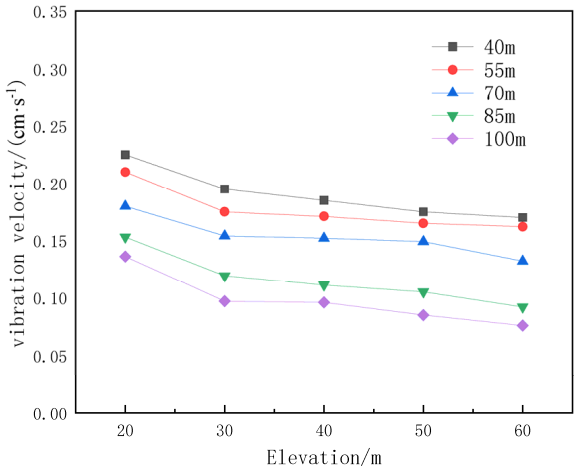

Figure 6. Horizontal tangent vibration velocity.

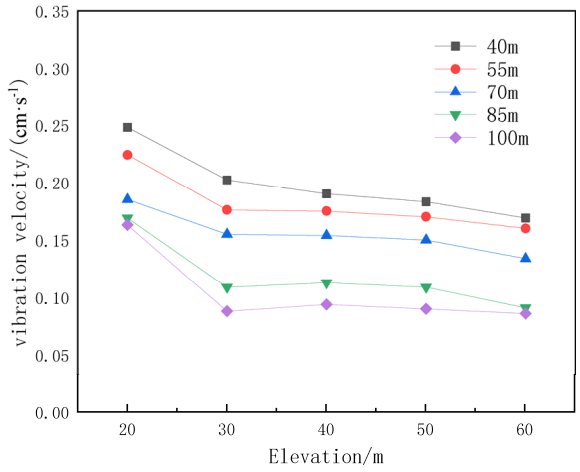

Figure 7. Vertical vibration velocity.

From Figures 5–7 above, it can be seen that the horizontal radial, tangential, and vertical vibration velocity with the increase in bench height is generally a decreasing trend. It decays faster in the early stage, slowly decays in the middle stage, and is relatively flat in the later stage. The least-squares fitting analysis yields vibration velocity and the relationship between the horizontal distance of the explosive center.

$$V = 0.53171 - 0.00705r + 3.61905E - 5r^2 \tag{10}$$

In this project, the maximum safe vibration velocity of the nearest residential building can be obtained by knowing the distance between the residential building and the explosive center.

3.4.2. Multivariate Linear Regression Analysis Using SPSS Software

(1) the establishment of multiple regression models

Equation (2) mainly responds to the blast vibration peak velocity, a single section of the maximum detonation charge and burst heart flat distance, and burst heart of the close relationship between the four, with a common form to express.

$$V = KQ^m R^n H^l \tag{11}$$

where m, n, and l are parameters that reflect the blasting method used, the geological conditions, and the ground conditions, respectively.

The multiple linear regression theory was used to establish a multiple linear regression equation for the decay of blasting seismic wave velocities, taking the logarithm of both sides of the above empirical equation to obtain the following function.

$$\ln V = \ln K + m \ln Q + n \ln R + l \ln H \tag{12}$$

Letting $\ln V = E(V)$, $\ln K = A$, $\ln Q = x_1$, $\ln R = x_2$, $\ln H = x_3$, gives the regression equation for its multiple linear regression model.

Therefore, the yield failure depth (h) of floor rock caused by stress concentration in coal seam mining can be obtained as follows.

$$E(V) = A + mx_1 + nx_2 + lx_3 \tag{13}$$

(2) Preprocessing of blast vibration measurement data

Table 3 is measured and preprocessed blast vibration data.

Table 3. Measured and preprocessed blast vibration data.

Frequency	Measurement Points	Horizontal Distance from the Explosive Center R(m)	Vertical Distance from the Explosive Center H(m)	Maximum Charge/Q (kg)	Peak vibration velocity/V (cm·s^{-1})	$E(V)$	x_1	x_2	x_3
1	No.1	40	60	18	0.171	−1.77	2.89	3.69	4.09
	No.2	55			0.162	−1.82		4.01	4.09
	No.3	70			0.134	−2.01		4.25	4.09
	No.4	85			0.093	−2.38		4.44	4.09
	No.5	100			0.086	−2.45		4.61	4.09

Table 3. *Cont.*

Frequency	Measurement Points	Horizontal Distance from the Explosive Center R(m)	Vertical Distance from the Explosive Center H(m)	Maximum Charge/Q (kg)	Peak vibration velocity/V ($cm \cdot s^{-1}$)	$E(V)$	x_1	x_2	x_3
2	No.1	40	50	18	0.183	−1.70	2.89	3.69	3.91
	No.2	55			0.17	−1.77		4.01	3.91
	No.3	70			0.15	−1.90		4.25	3.91
	No.4	85			0.111	−2.20		4.44	3.91
	No.5	100			0.095	−2.35		4.61	3.91
3	No.1	40	40	18	0.19	−1.66	2.89	3.69	3.69
	No.2	55			0.175	−1.74		4.01	3.69
	No.3	70			0.154	−1.87		4.25	3.69
	No.4	85			0.115	−2.16		4.44	3.69
	No.5	100			0.105	−2.25		4.61	3.69
4	No.1	40	30	18	0.202	−1.60	2.89	3.69	3.40
	No.2	55			0.176	−1.74		4.01	3.40
	No.3	70			0.155	−1.86		4.25	3.40
	No.4	85			0.12	−2.12		4.44	3.40
	No.5	100			0.108	−2.23		4.61	3.40
5	No.1	40	20	18	0.31	−1.17	2.89	3.69	3.00
	No.2	55			0.25	−1.39		4.01	3.00
	No.3	70			0.21	−1.56		4.25	3.00
	No.4	85			0.204	−1.59		4.44	3.00
	No.5	100			0.184	−1.69		4.61	3.00

(3) Regression analysis

The dependent variable is $E(V)$. The independent variables are x_1, x_2, and x_3. Since the maximum amount of material in a single section remains the same when blasting, only x_2 and x_3 are considered as independent variables, which are analyzed by ordinary linear regression using SPSS software to establish a multiple linear regression model. The test of the regression model consisted of three aspects: a significance test of the multiple linear regression equation, the regression coefficients, and the goodness of fit. Table 4 shows the model summary, which summarizes the approximate model fit of the surface model.

Table 4. Summary of models [C].

Model	R	R^2	Adjusted R^2	Errors in Standard Estimation	Change of statistics					
					Amount of Change in the R^2	Amount of Change of F	Degree of Freedom 1	Degree of Freedom 2	Significant Amount of F Change	Durbin Watson
1	0.940 [b]	0.884	0.874	0.11496	0.884	83.918	2	22	0.000	0.974

The [C] represents the dependent variable $E(V)$, and [b] represents the constants x_1,x_2.

① The better the fit (R^2) is, the better the fit of the regression equation to the sample observations, which is usually tested by the sample coefficient of determination. R^2 is in the closed interval between 0 and 1, and the closer its value is to 1, the better the fitting effect; the closer it is to 0, the worse the fit. As can be seen from Table 4: R^2 = 0.884 and

the adjusted value R^2 = 0.874, indicating that the regression equation is a good fit for the sample observations.

② Analysis of variance (ANOVA). The regression fitting process of ANOVA results are shown in Table 5. The f-test is a significance test of the regression equation, indicating the degree of combined influence of multiple factors, the significance value less than 0.05 to be meaningful. SPSS software for the model for the F-test, and the significance value of 0.000 b, less than 0.05, indicating that the burst heart flat distance, burst vertical distance from the overall of the dependent variable peak vibration speed has a significant impact, the overall regression equation is significant, there is a linear relationship, statistically significant, but does not reflect the strength of each independent variable on the overall impact. A statistically significant model does not mean that all the variables within the model are statistically significant and further testing of the respective variables is required.

Table 5. Analysis of variance.

Model	Quadratic Sum	Freedom	Mean Square	F	Significance
regression	2.218	2	1.109	83.918	0.000 [b]
Residuals	0.291	22	0.013		
Total	2.509	24			

The [b] represents the constant x_2.

③ Estimation of regression coefficients. The valuation of the model regression coefficients is shown in Table 6, and substituting the values from Tables 3 and 6 into Equation (13) yields, m = −0.0018, so the multiple linear regression equation is as follows.

$$E(V) = 2.864 - 0.0018x_1 - 0.701x_2 - 0.498x_3 \quad (14)$$

where $E(V)$ is the dependent variable and represents the ln value of the peak vibration velocity; x_1 represents the effect of the maximum amount of material in a single section on the peak vibration velocity; x_2 represents the effect of the flat distance from the burst center on the peak vibration velocity; x_3 represents the effect of the vertical distance from the burst center on the peak vibration velocity.

Table 6. Peak vibration speed regression coefficients.

Model	Unstandardized Factor		Standardization Factor	t	Significance	Tolerance	VIF
	B	Standard Errors	Beta				
(Constants)	2.864	0.368		7.780	0.000		
lnR	−0.701	0.071	−0.716	−9.861	0.000	1.000	1.000
lnH	−0.498	0.059	−0.610	−8.403	0.000	1.000	1.000

④ Regression coefficients as well as significance tests, t-test is a test of significance for individual independent variables. After the t-test, the significance *p*-value of the burst heart flat distance and burst heart vertical distance did not exceed 1, indicating a significant effect on the regression equation, which is statistically significant and cannot be excluded from the regression equation.

⑤ Variance inflation factor (VIF), the value is the inverse of tolerance, the larger the value of VIF, the more serious the covariance problem, when VIF > 10, there is a strong covariance problem. Since the VIF of the burst heart flat distance and burst heart flat are 1.000, there is no covariance between the model independent variables.

⑥ Analysis of residuals. The purpose of residual analysis is to check and ensure the quality of the test data and to diagnose the effect of the regression. In regression analysis, there is a category of test values that are outliers, which are far from other values and show a large residual, affecting the effect of the fit of the regression equation. As can be seen from Table 7: standard residuals less than 3 and standard predicted values less than 3 indicate that none of the observed data are outliers and will not affect the regression equation fitting effect.

Table 7. Residual statistics.

-	Minimum Value	Maximum Value	Average	Standard Deviations	No. of Cases
Predicted values	−2.4012	−1.2122	−1.8793	0.30401	25
Residuals	−0.18534	0.16341	0.00000	0.11007	25
Standard predicted values	−1.717	2.194	0.000	1.000	25
Standard residuals	−1.612	1.421	0.000	0.957	25

⑦ Scatterplot of regression residuals. Figure 8 shows a scatter plot of the standardized residuals of the regression. As can be seen in Figure 8: the residuals are generally normally distributed and the multiple linear regression equation is a good fit.

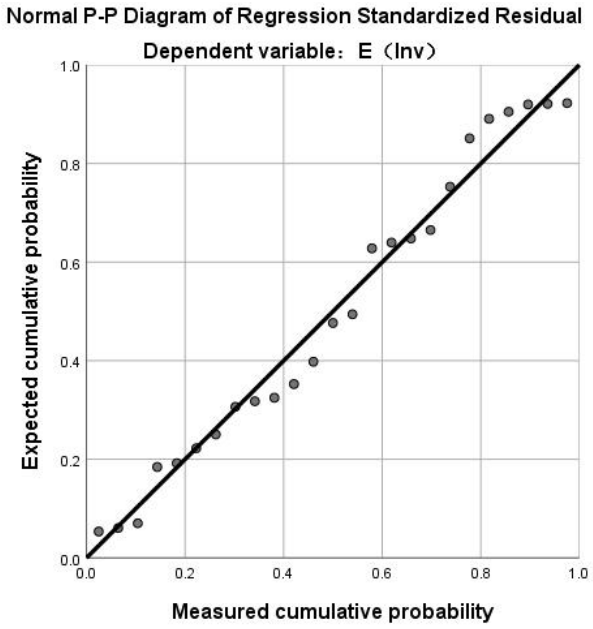

Figure 8. Scatterplot of regression-standardized residuals.

The R-test values, F-test values, and *p*-test values indicate that the dependent variable lnV has a significant linear correlation with the independent variables lnR and lnH. The regression coefficients A = 2.864, m = −0.0018, *n* = −0.701, l = −0.498 can be obtained from Table 6, which can be solved by substituting into Equation (11).

$$V = 17.53 \frac{Q^{-0.0018}}{R^{0.701} \cdot H^{0.498}} \tag{15}$$

Therefore, the conclusion drawn from the multiple linear regression model analysis is that the blast vibration speed is affected by two main factors, which are horizontal distance from the explosive center and vertical distance from the explosive center. Since the absolute value of the standard regression coefficient reflects the degree of impact on blast vibration, the larger the absolute value, the greater the performance of the control. From Table 6, it can be seen that the horizontal distance from the explosive center on the degree of impact of blast vibration is greater than the burst center vertical distance, the overall peak vibration speed with horizontal distance from the explosive center and vertical distance from the explosive center increases and tends to decay.

The peak vibration velocity propagation laws in the three directions in the results of this section are basically consistent with the results of previous related studies. The horizontal radial, tangential, and vertical vibration velocity with the increase in bench height is generally a decreasing trend. It decays faster in the early stage, slowly decays in the middle stage, and is relatively flat in the later stage. The influence of the horizontal distance of the blast center on the blasting vibration is greater than that of the vertical distance of the blast center.

4. Numerical Simulation Analysis of Blasting Dynamic Effect

4.1. Numerical Model and Material Parameters

(1) Numerical model

As the maximum vibration velocity occurs at the source of the blast at an elevation of 20 m, it is established at an elevation of 20 m with the numerical model. The total bench height of the model is 40 m, and the explosive source elevation is 20 m. The total length is 150 m, the thickness of the rock layer perpendicular to the paper surface is 20 m, and the height of the segmental bench is 10 m, the slope angle of the bench is 70°, the depth of the hole is 9 m, the diameter of the hole is 70 mm, and the fill is 3 m. The Lagrange grid is used to mesh the rock and fill parts, and the ALE grid is used to mesh the explosives part. The 3D-SOLID164 solid unit was used for the calculation, and the m-kg-s unit system was used for the numerical model. In order to identify the intrinsic link between blasting vibration velocity and stress field under bench blasting, five measurement points at the same horizontal direction as the site monitoring point arrangement and at an elevation of 20 m were selected for analysis during the simulation, as shown in Figure 9.

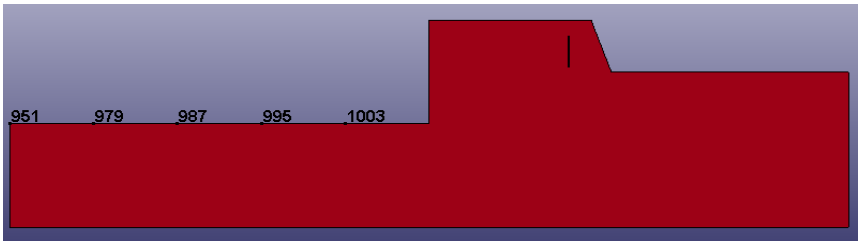

Figure 9. Layout of monitoring points at an elevation of 20 m.

(2) State equation

Modeling the relationship between pressure and specific volume during blasting using the JWL (Jones–Wilkens–Lee) state equation.

$$P = A(1 - \frac{\omega}{R_1 V})e^{-R_1 V} + B(1 - \frac{\omega}{R_2 V})e^{-R_1 V} + \frac{\omega E}{V} \quad (16)$$

where P is pressure; V is relative volume; E is initial specific internal energy; ω, A, B, R_1, and R_2 are material constants.

(3) Explosive material

The explosive used in this simulation is an emulsion explosive, and emulsion explosive performance parameters are shown in Table 8.

Table 8. Emulsion explosive performance parameters.

Material	ρ/kg·m^{-3}	D /m·s^{-1}	$P_{c\text{-}j}$/Pa	A	B	R_1	R_2	ω	E_0 /Pa	V_0
Emulsion explosive	1.20×10^3	3.50×10^3	6×10^9	2.1444×10^{11}	1.82×10^8	4.2	0.9	0.15	4.19×10^8	1

(4) Rock material

The relevant parameters of rock materials used in this simulation are shown in Table 9.

Table 9. Physical and mechanical parameters of rock.

Material	Density/kg·m^{-3}	Elastic Modulus /Pa	Poisson's Ratio	Compressive Yield Strength /Pa	BETA	FS
Rock	2200	2×10^9	0.3	7×10^7	1	0.8

(5) Filling material

The SOIL_AND_FOAM material model was selected as the fill material based on the rock dust and clay from the borehole used for filling the sandstone mine site, with the main parameters shown in Table 10.

Table 10. Calculation parameter table of filling materials.

Material	Density/kg·m^{-3}	Shear Modulus /Pa	Bulk Modulus/Pa	A0	A1	A2	PC
Soil	1800	7.8×10^6	2.4×10^9	2.7×10^{-3}	1.3×10^{-7}	0.12	0

4.2. Analysis of Dynamic Effects

According to the above model of the arrangement of monitoring points, the elevation of 20 m, different horizontal distances from the explosive center of the velocity response for analysis, so selects the bench height of 20 m, horizontal distance from the explosive center of 40 m, 55 m, 70 m, 85 m, 100 m, respectively. Five measurement points at each direction and synthesis of the velocity change with a time curve graph of vibration velocity are shown in Figure 10.

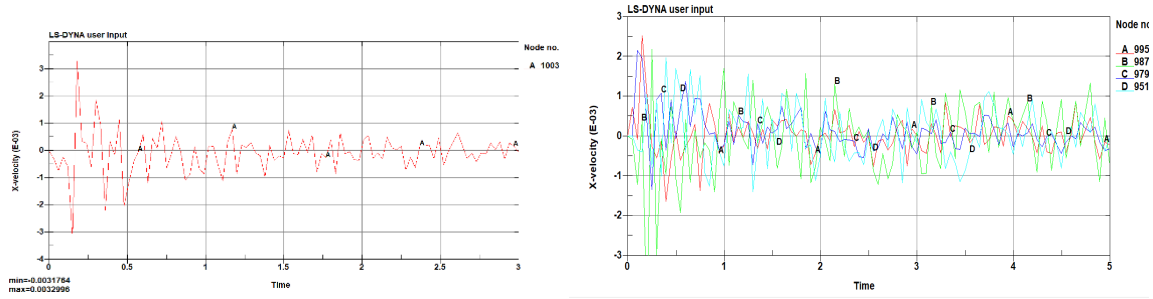

(**a**) Horizontal radial nodal vibrational velocity time course graph.

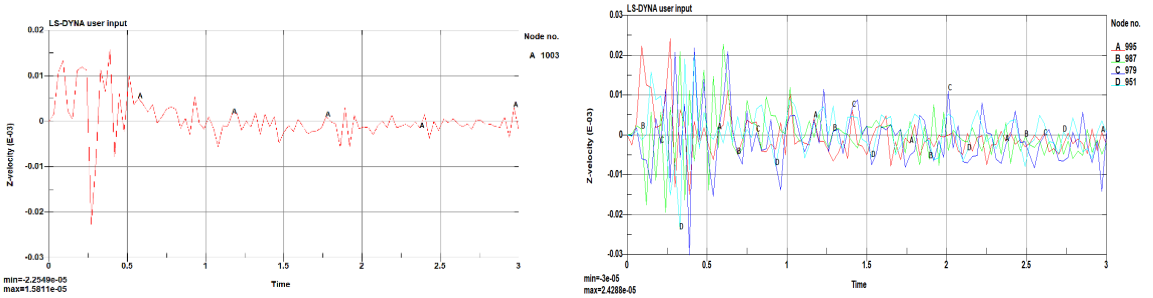

(**b**) Horizontal tangential nodal vibrational velocity time course graph.

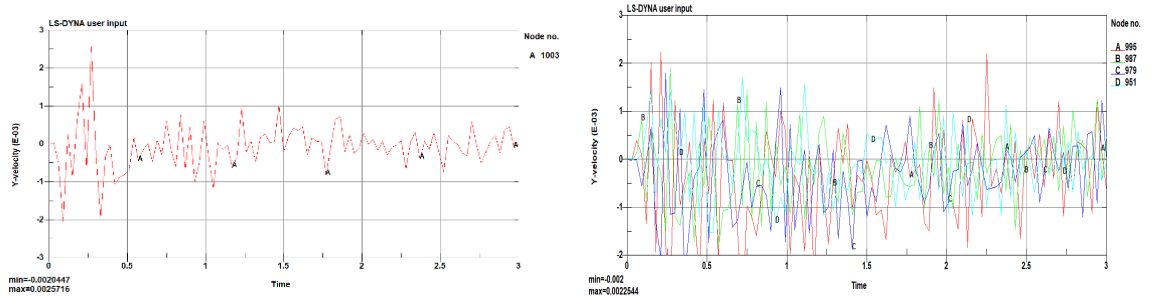

(**c**) Vertical nodal vibrational velocity time course graph.

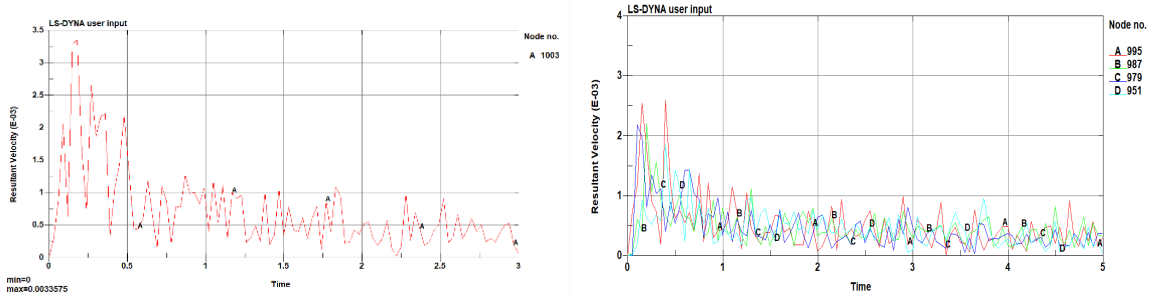

(**d**) Time course diagram of nodal three directions resultant vibration velocity.

Figure 10. Time course diagram of nodal vibrations at different horizontal distances for an elevation of 20 m.

From the numerical calculation of the dynamic response results, Figure 10 shows the nodal vibration velocity time course diagram at different horizontal distances, Figure 11 shows the tangential velocity cloud at different time nodes; Figure 12 shows the synthetic velocity cloud, as the model is a symmetrical boundary condition, the constraint imposed is that the displacement in the Z direction is zero, i.e., the vibration velocity and acceleration in the Z direction are zero, the five measurement points are in the same horizontal direction whether in the field test or in the numerical model velocity in the Z direction are close to zero, and the velocity in the Z direction (tangential) is not compared to the relative error, as shown in Table 11.

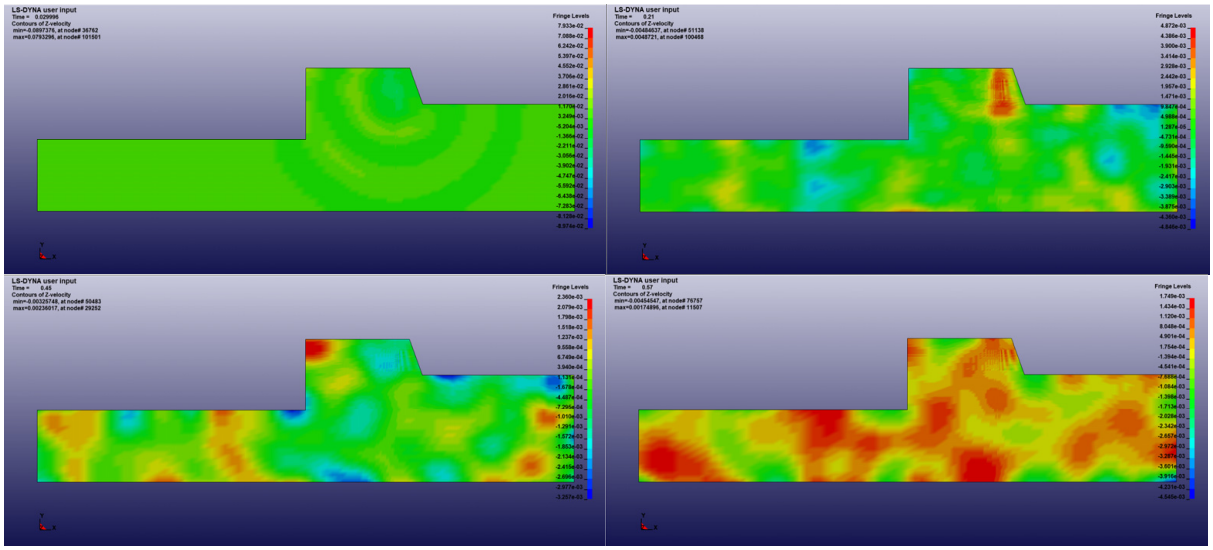

Figure 11. Tangential velocity clouds at different time points for an elevation of 20 m.

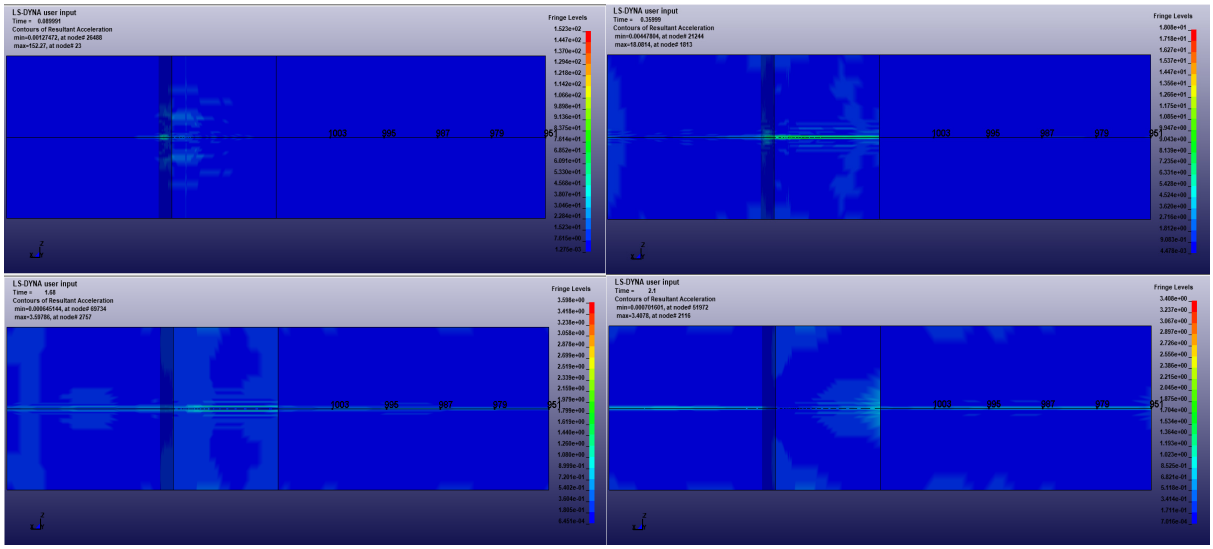

Figure 12. Nodal resultant velocity overhead clouds at different times for an elevation of 20 m.

Table 11. Comparison of numerical results and measured values for an elevation of 20 m.

Measuring Point /Nodal Point	Numerical Results V_2/(cm·s^{-1})				Measured Values V_1/(cm·s^{-1})				Relative Error $\lvert V_1/V_2-1\rvert\times100\%$		
	Radial Direction	Vertical Direction	Tangential Direction	Resultant Velocity	Radial Direction	Vertical Direction	Tangential Direction	Total	Radial Direction	Vertical Direction	PEAK VALUE
1/A	0.329	0.257	0.016	0.336	0.310	0.248	0.225	0.310	5.77	3.5	7.74
2/A	0.252	0.225	0.024	0.260	0.250	0.224	0.210	0.250	0.8	0.4	3.8
3/B	0.218	0.190	0.023	0.221	0.210	0.185	0.180	0.210	3.6	2.6	4.9
4/C	0.215	0.182	0.022	0.219	0.204	0.169	0.153	0.204	5.99	7.7	6.8
5/D	0.197	0.170	0.020	0.186	0.184	0.163	0.136	0.184	6.6	4.1	1.07

4.3. Comparison Analysis between Numerical Simulation Results and Field Measurements

The comparison of the numerical simulation results with the peak vibration speed of the field test and plotting its variation on a line graph, is shown in Figure 13.

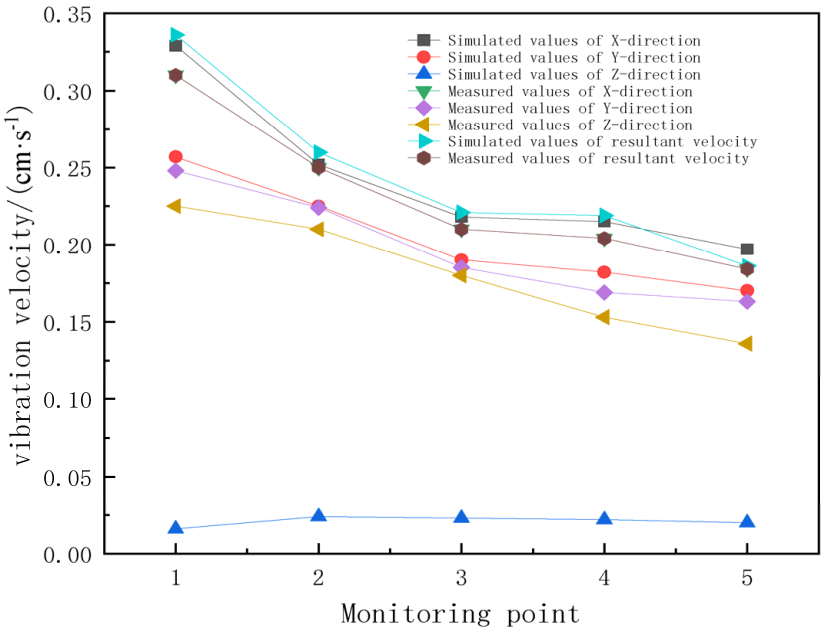

Figure 13. Comparison of numerical results with measured values for an elevation of 20 m.

As can be seen from Table 6 and Figure 13, the numerical simulation results are generally greater than the field test vibration velocity data results, and their relative errors are all below 10%, and three directions peak vibration velocity decay trends do not differ much and remain basically the same. Since the numerical simulation ignores the internal structure of the actual rock mass, it simplifies the model as a continuous medium, and does not consider the influence of rock fracture zones, topography, and discontinuous surfaces, etc., thus making the numerical simulation calculation results generally greater than the results of field test monitoring. The relative error in the horizontal radial direction is basically greater than the error in the vertical direction, but the total error is not large. The peak vibration velocity in all three directions decay strictly with increasing the horizontal distance of the explosive center, and are basically consistent with field measurements.

Analysis of the shear stress response of the five measurement points and the field actual measurement program to maintain consistency with the corresponding unit as shown in Figure 14, respectively, units 6339, 6179, 6019, 5859, 5699, extract the maximum shear stress in its five units with time data, as shown in Figure 15.

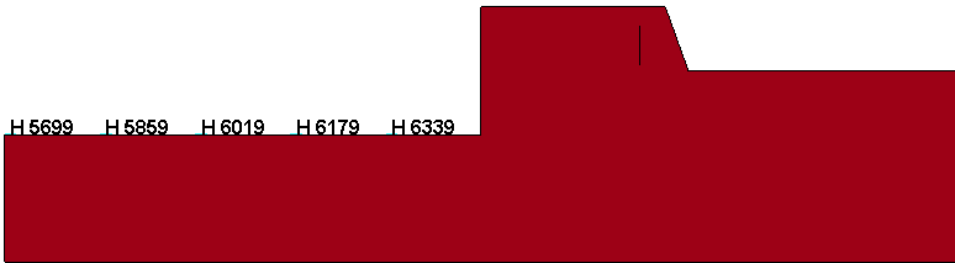

Figure 14. Layout of the horizontal radial monitoring point is located at an elevation of 20 m.

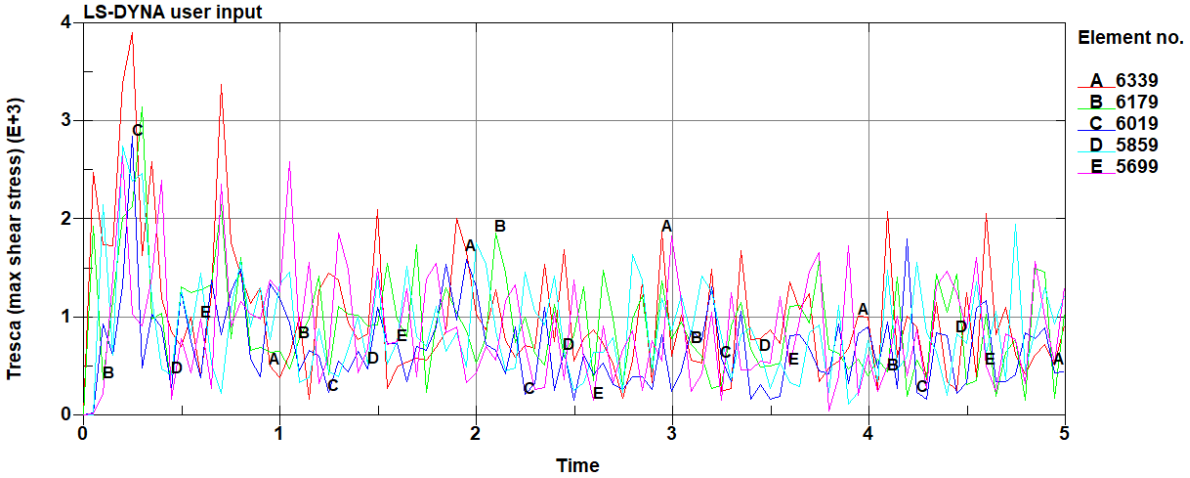

Figure 15. Cloud of maximum shear stress for an elevation 20 m.

According to the above maximum stress time curve in Figure 15, the peak shear stress of each unit is extracted as shown in Table 12 and its trend is shown in Figure 16.

Table 12. The peak horizontal radial shear stress at an elevation of 20 m.

Monitoring Points	1	2	3	4	5
Peak shear stress/kPa	3.91	3.15	2.85	2.75	2.60

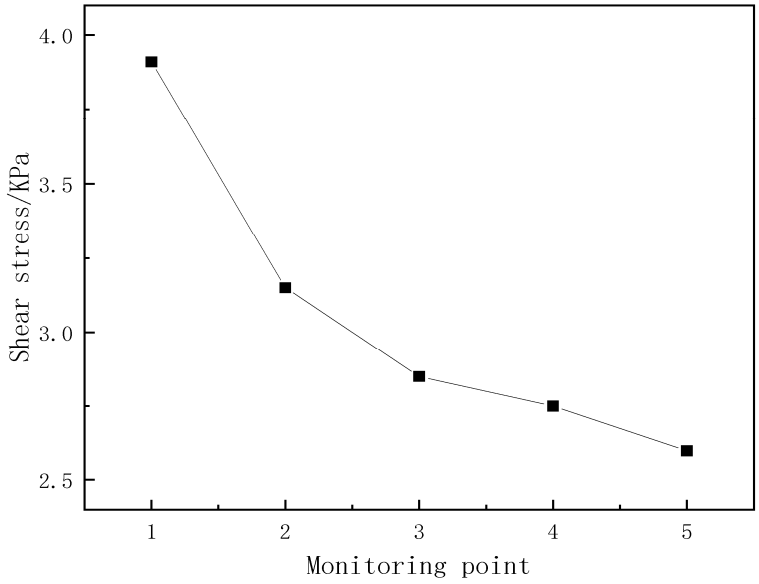

Figure 16. Peak horizontal radial shear stress diagram at an elevation of 20 m.

In summary, the elevation is 20 m, five monitoring points of the horizontal shear stress and vibration velocity decay strictly with an increasing horizontal distance from the explosive center, shear stress decays faster in the near zone of the source and slower in the far area, maybe in blasting seismic wave propagation to the residential house, the complex geological structure changes its propagation direction, and the energy attenuation caused, in order to explore the relationship between the horizontal radial shear stress and the peak vibration velocity, so non-linear fitting analysis is used, as shown in Figure 17.

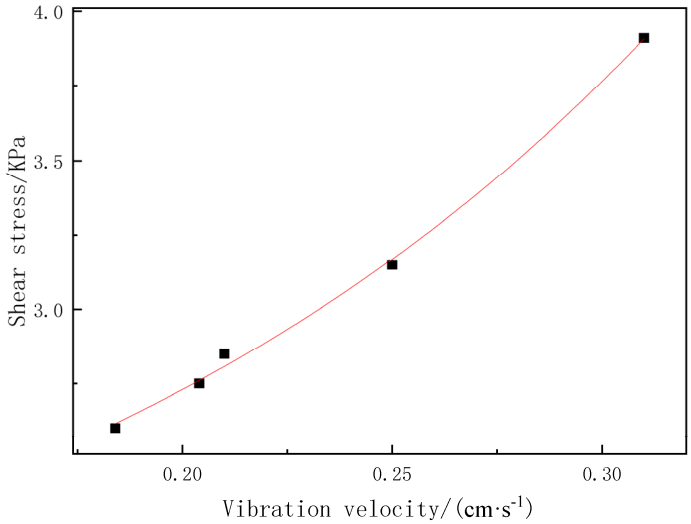

Figure 17. Horizontal radial peak shear stress versus synthetic peak vibration at an elevation of 20 m velocity.

The relationship between the horizontal radial peak shear stress and the composite peak vibration velocity is obtained from the fitting analysis is as follows.

$$\tau = 2.14829 - 1.21417v + 19.24462v^2 \quad (R^2 = 0.99594) \tag{17}$$

According to the safety regulations for blasting (GB6722-2014), the relationship between shear stress and vibration velocity can be combined to determine whether the blast exceeds the range of safety regulations and the shear strength of the building. Then, the nature of the structural material is used to determine whether the building is damaged or destroyed, providing a reference for blast vibration control, hole net parameters, and design indicators.

The changes of peak vibration velocity and shear stress in the results of this section are basically consistent with the results of previous related studies. It can be seen from the chart and table that the numerical simulation results are generally greater than the field test vibration velocity data results, and their relative errors are all below 10%.

5. Conclusions

In this study, based on the field measurement data of the bench blasting vibration, the peak vibration velocity of the measurement point is comprehensively analyzed. The comparison and verification are carried out with the numerical simulation method. The vibration propagation law and dynamic effect of bench blasting obtained from the measured values and numerical results are consistent.

(1) The peak vibration velocity in all three directions decays strictly with increasing elevation and horizontal distance. The elevation correction formula proposed by CRSRI and the least-squares method are used to perform regression analysis of the monitoring data. An empirical formula for peak vibration velocity attenuation is established. According to the safety regulations for blasting (GB6722-2014), the safe vibration velocity was no more than 1.5 cm/s, and the civil house was in a safe state. Fitting analysis to obtain the peak vibration velocity and the relationship between the horizontal distance from the explosive center can determine whether blasting vibration occurs on the adjacent buildings.

(2) Shear stress decreases strictly with increasing horizontal distance of the explosive center, shear stress and vibration velocity decay faster in the near zone of the source and slower in the far area.

(3) The analysis found a quadratic, exponential relationship between shear stress and vibration velocity, and the research results can be used as a safety criterion for buildings

under the action of blasting, providing a reference for blasting vibration control, hole net parameters, and design indicators.

(4) SPSS statistical software is applied to the parameters of the multiple linear regression analysis, the peak vibration speed of the multiple linear regression equation, the establishment of the peak vibration speed of the regression model. Through the regression model for F-test, t-test, and regression diagnosis, we determined that there is no co-linearity between the flat distance of the burst core and the vertical distance of the burst core, and its overall impact on the regression equation and regression coefficient is significant, the multiple linear regression equation fits well, and the use of multiple linear regression analysis model can predict the change of mass vibration intensity relatively accurately.

The finite element method in the numerical simulation has a certain limitation to simulate the practice situations of background engineering. In addition, further research should also consider the influence of blasting vibration frequency and the internal structure of rock mass on the strength of blasting vibration, especially the rock mass containing karst caves.

Author Contributions: L.H.: Formal analysis, Numerical simulation, Field monitoring, Writing—Original draft; D.K.: Data curation, Methodology, Writing—Original draft, Numerical Simulation, Funding acquisition, Writing—Review and editing; Z.L.: Numerical simulation, Field monitoring. All authors have read and agreed to the published version of the manuscript.

Funding: This research was funded by the National Natural Science Foundation of China (No. 52164002, 52164005, 52064005 and 51904082); and the New Engineering Research and Practice Project (E-KYDZCH20201822).

Institutional Review Board Statement: Not applicable.

Informed Consent Statement: Not applicable.

Data Availability Statement: All data used during the study appear in the submitted article.

Acknowledgments: The authors would also like to thank the editors and anonymous reviewers for their valuable time and suggestions.

Conflicts of Interest: The authors declare that they have no conflict of interest.

References

1. Jain, A.S.; Tippur, H.V. Extension of reflection-mode digital gradient sensing method for visualizing and quantifying transient deformations and damage in solids. *Opt. Lasers Eng.* **2016**, *77*, 162–174. [CrossRef]
2. Javed, R.A.; Zhu, S.F.; Guo, C.H.; Jiang, F.C. Analyzing Stress Wave Propagation in a Hollow Bar Loaded Three-Point Bend Fracture Test Using Numerical Methods. *Appl. Mech. Mater.* **2015**, *782*, 252–260. [CrossRef]
3. Spathis, A.T. Frequency dependent damage criteria for ground vibrations produced by blasting. In *Rock Fragmentation by Blasting*; China Metallurgical Industry Press: Beijing, China, 2002; pp. 582–590.
4. Yin, Z.-Q.; Hu, Z.-X.; Wei, Z.-D.; Zhao, G.-M.; Hai-Feng, M.; Zhang, Z.; Feng, R.-M. Assessment of blasting-induced ground vibration in an open-pit mine under different rock properties. *Adv. Civ. Eng.* **2018**, *2018*, 4603687. [CrossRef]
5. Yu, M.; Lin, C.M.; Chang, F.Q.; Ying, R.P. Research on Amplification Effect of Blasting Vibration in Rock Deep Foundation Pit. *Blasting* **2017**, *34*, 27–32, 65. [CrossRef]
6. Tang, H.; Li, H.B. Study of blasting vibration formula of reflecting amplification effect on elevation. *Rock Soil Mech.* **2011**, *32*, 820–824. [CrossRef]
7. Li, X.; Li, Q.; Hu, Y.; Chen, Q.; Peng, J.; Xie, Y.; Wang, J. Study on Three-Dimensional Dynamic Stability of Open-Pit High Slope under Blasting Vibration. *Lithoshere* **2022**, *2021*, 6426550. [CrossRef]
8. Wan, S.; Li, H. *Study of blasting seismic effects of underground powerhouse of pumped storage project in granite condition. IOP Conference Series: Materials Science and Engineering*; IOP Publishing: Bristol, UK, 2018; Volume 322, p. 042033. [CrossRef]
9. Rodríguez, R.; de Marina, L.G.; Bascompta, M.; Lombardía, C. Determination of the ground vibration attenuation law from a single blast: A particular case of trench blasting. *J. Rock Mech. Geotech. Eng.* **2021**, *13*, 1182–1192. [CrossRef]
10. Zhu, J.; Wei, H.; Yang, X.; Chu, H. Prediction of blasting vibration velocity of layered rock mass under multihole cut blasting. *Shock. Vib.* **2021**, *2021*, 5511190. [CrossRef]
11. Chen, L.; Chen, J.; Luo, Y.; Guo, Y.; Mu, Y.; Zhong, D.; Liu, W.; Yang, T.; Chen, W. Propagation laws of blasting seismic waves in weak rock mass: A case study of muzhailing tunnel. *Adv. Civ. Eng.* **2020**, *2020*, 8818442. [CrossRef]

12. Lin, F.; Liu, R.; Zhang, Z.; Jiang, D.; Chen, J.; Li, Y. Reduction of blasting induced ground vibrations using high-precision digital electronic detonators. *Front. Earth Sci.* **2022**. [CrossRef]
13. Xiao, Y.-G.; Cao, J.; Liu, X.-M.; Li, C.-H. Effect of Open-Pit Blasting Vibrations on a Hanging-Wall Slope: A Case Study of the Beizhan Iron Mine in China. *Geofluids* **2022**, *2022*, 6943834. [CrossRef]
14. Gao, J.; Huang, C.; Huang, X.; Ren, J.-J.; Wang, N. A Study of Blast Vibration Propagation Law under Negative Altitude Terrains. *Math. Probl. Eng.* **2022**, *2022*, 4289057. [CrossRef]
15. Zhang, C.; Ge, Y.; Lv, J.; Ren, G. Study on elevation effect of blast wave propagation in high side wall of deep underground powerhouse. *Bull. Eng. Geol. Environ.* **2021**, *80*, 3973–3987. [CrossRef]
16. Tian, X.; Song, Z.; Wang, J. Study on the propagation law of tunnel blasting vibration in stratum and blasting vibration reduction technology. *Soil Dyn. Earthq. Eng.* **2019**, *126*, 105813. [CrossRef]
17. Yan, B.; Liu, M.; Meng, Q.; Li, Y.; Deng, S.; Liu, T. Study on the Vibration Variation of Rock Slope Based on Numerical Simulation and Fitting Analysis. *Appl. Sci.* **2022**, *12*, 4208. [CrossRef]
18. Xie, B.; Zhang, X.; Wang, H.; Jiao, Y.; Zheng, F. Investigations into the Rock Dynamic Response under Blasting Load by an Improved DDA Approach. *Adv. Civ. Eng.* **2021**, *2021*, 8827022. [CrossRef]
19. Deng, X.; Wang, J.; Wang, R.; Liu, Q. Influence of blasting vibrations generated by tunnel construction on an existing road. *Int. J. Civ. Eng.* **2020**, *18*, 1381–1393. [CrossRef]
20. Khandelwal, M.; Singh, T.N. Prediction of blast induced ground vibrations and frequency in opencast mine: A neural network approach. *J. Sound Vib.* **2006**, *289*, 711–725. [CrossRef]
21. Shang, Y.; Kong, D.; Pu, S.; Xiong, Y.; Li, Q.; Cheng, Z. Study on Failure Characteristics and Control Technology of Roadway Surrounding Rock under Repeated Mining in Close-Distance Coal Seam. *Mathematics* **2022**, *10*, 2166. [CrossRef]
22. Li, H.; Dong, W.Z. The Blasting Test with Precise Delayed Time Interval and Wavelet Pocket Analysis for Vibration Signals' Energy. *Adv. Mater. Res.* **2014**, *1023*, 198–204. [CrossRef]
23. Hajihassani, M.; Armaghani, D.J.; Monjezi, M.; Mohamad, E.T.; Marto, A. Blast-induced air and ground vibration prediction: A particle swarm optimization-based artificial neural network approach. *Environ. Earth Sci.* **2015**, *74*, 2799–2817. [CrossRef]
24. Amiri, M.; Amnieh, H.B.; Hasanipanah, M. A new combination of artificial neural network and K-nearest neighbors models to predict blast-induced ground vibration and air-overpress. *Eng. Comput.* **2016**, *32*, 631–644. [CrossRef]
25. Liu, H.; Fu, J.; Ning, J. Experimental Study on the Dynamic Mechanical Properties of Reinforced Concrete under Shock Loading. *Acta Mech. Solida Sin.* **2016**, *29*, 22–30. [CrossRef]
26. Bacon, C. Separation of waves propagating in an elastic or viscoelastic Hopkinson pressure bar with three-dimensional effects. *Int. J. Impact Eng.* **1999**, *22*, 55–69. [CrossRef]
27. Lei, Z.; Kang, Q.; Zhao, M.S.; Chi, E.N. Numerical Simulation and Experimental Study on Vibration-Decreasing Function of the Barrier Holes. *Appl. Mech. Mater.* **2014**, *602–605*, 53–59. [CrossRef]
28. Zhang, Z.; Zhou, C.; Remennikov, A.; Wu, T.; Lu, S.; Xia, Y. Dynamic response and safety control of civil air defense tunnel under excavation blasting of subway tunnel. *Tunn. Undergr. Space Technol.* **2021**, *112*, 103879. [CrossRef]
29. Wu, X.; Zhang, Y.; Guo, Q. Influence of the step elevation on blasting seismic wave. *Appl. Mech. Mater.* **2016**, *4299*, 131–136. [CrossRef]
30. Yang, J.; Xia, Y.; Chen, Z.; Chen, D.; Pei, Y.; Zhu, W. Dynamic Behavior of Road High Cutting Rock Slope under the Influence of Blasting for Excavation. *Procedia Earth Planet. Sci.* **2012**, *5*, 25–31. [CrossRef]
31. Blair, D.P. Dynamic response of mine pit walls. *Int. J. Rock Mech. Min. Sci.* **2018**, *106*, 14–19. [CrossRef]
32. Jiang, N.; Zhu, B.; Zhou, C.; Li, H.; Wu, B.; Yao, Y.; Wu, T. Blasting vibration effect on the buried pipeline: A brief overview. *Eng. Fail. Anal.* **2021**, *129*, 105709. [CrossRef]
33. Esmatkhah Irani, A.; Azadi, A.; Nikbakht, M.; Azarafza, M.; Hajialilue Bonab, M.; Behrooz Sarand, F. GIS-based Settlement Risk Assessment and its Effect on Surface Structures: A Case Study for the Tabriz Metro—line 1. *Geotech. Geol. Eng.* **2022**, 1–22. [CrossRef]
34. Chaudhary, R.K.; Mishra, S.; Chakraborty, T.; Matsagar, V. Vulnerability analysis of tunnel linings under blast loading. *Int. J. Prot. Struct.* **2019**, *10*, 73–94. [CrossRef]
35. Tsang, H.H.; Gad, E.F.; Wilson, J.L.; Jordan, J.W.; Moore, A.J.; Richards, A.B. Mine blast vibration response spectrum for structural vulnerability assessment: Case study of heritage masonry buildings. *Int. J. Archit. Herit.* **2018**, *12*, 270–279. [CrossRef]